Integrated monitoring of atmospheric aerosol vertical profiles using LIDAR and MAX-DOAS

Jihyo Chong, Dong Ho Shin, and Young J. Kim*
Advanced Environmental Monitoring Research Center, School of Environmental Science and Engineering,
Gwangju Institute of Science and Technology, 1 Oryong dong, Buk-gu, Gwangju 500-712, Korea
*corresponding author: yjkim@gist.ac.kr

INTRODUCTION

Information on the vertical distribution of aerosols is important for understanding their transport characteristics as well as radiative effect. In order to establish effective control strategies for aerosols in areas of interest, it is important to understand their chemical and physical properties including spatial and temporal distributions in the atmosphere. Ground-based measurements of tropospheric aerosol using a MAX-DOAS system and a multi-wavelength Raman lidar system were conducted 28~30 May and 4~8 June 2005 at the Korea Global Atmosphere Watch Observatory (KGAWO) (36.56◦N, 126.47◦E), located in Anmyeon Island off the west coast of Korea.

MEASUREMENT & METHOD

MAX-DOAS measurements were conducted between 06:00 Local Time (LT) and 18:00 LT on the rooftop of the KGAWO building (43 m above sea level) during daytime. The viewing azimuth angle of the MAX-DOAS telescope was 340◦, pointing east to the Yellow Sea. The GIST multi-wavelength Raman lidar system was used to evaluate the performance of MAX-DOAS aerosol measurements. The lidar system utilizes aNd:YAGlaser as a light source, which emits pulses at wavelengths of 355, 532, and 1064 nm.

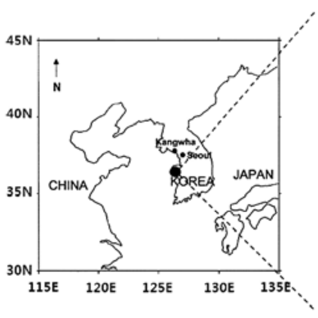

Figure 1. Site information

Fig.2. MAX-DOAS system

Fig.3. Mobile Lidar system

Table 1. Measurement parameters of MAX-DOAS system and Lidar system specifications

When	28 May – 8 June 20
Where	Anmyeon Island, Korea (Korea GAW site)
Target species	Aerosol vertical distribution [O_4]
Instrument-ation	MAX-DOAS system
Elevation angles	3º, 5º, 10º, 15º, 20º, 90º (each sequence takes ~20 min)
Wavelength range	298 ~ 431 nm

Lidar system specifications		
Laser	Type	Nd:YAG Laser Continuum Surelite III-10
	Wavelength and Pulse energy	140 mJ (at 355 nm), 154 mJ (at 532 nm) and 640 mJ (at 1064 nm)
	Beam Divergence	0.2 mrad after 5X beam expansion
	Repetition rate	10Hz
	Pulse duration	<10 ns
Receiver optics	Optical design	Schmidt–Cassegrain telescope 14-inch
	Focal length	3910 mm (14 inch telescope)
	Field of view	0.5–4.0 mrad (variable)
Dispersion system	Wavelength (nm)	355, 360, 387, 407, 532parallel, 532vertical, 546, 607, 1064
	Bandwidth (nm) of interference filter	355, 360, 387, 407, 532parallel, 532vertical, 546, 607, 1064 5, 3, 0.72, 0.97, 1, 1, 3, 0.45, 1
Data acquisition system	Detector	PMT (HAMAMATSU R3234-01) for 355, 360, 387, 407, 532, 546, 607 nm channel; HAMAMATSU R3236 for 1064 nm channel
	Photon counting Maximum count rate	MCS PCI Photon counting 150 MHz (15 m vertical resolution)

ANALYSIS

O4 SCDs were retrieved using the evaluation software WinDOAS V2.10. The spectra collected by the MAX-DOAS system were pre-calibrated using mercury lamp signals from which dark current and offset signals were subtracted. The pre-calibrated spectra were calibrated again by fitting them to a solar reference spectrum. A 5th-order polynomial fit was used to remove broadband structures and the effects of Rayleigh and Mie scattering. The O4 SCDs were determined in the spectral range from 338 to 367 nm. The spectrum taken at around noon on 30 May was used as a Fraunhofer reference spectrum (FRS), using the nonlinear least squares method

Table 2. Summary of MAX-DOAS Specification

Subject	Setting
Reference spectrum	Spectrum measured at noon
Cross-sections	NO_2, O_4, O_3, HCHO, Ring, FRS
Fitting window	338-367 nm
Polynomial order	5

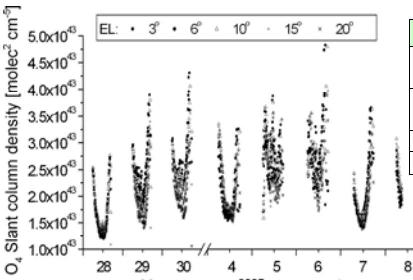

Figure 4. Temporal variations in O4 SCD values obtained at EL = 3◦, 6◦, 10◦, 15◦, and 20◦ during measurement period (28–30 May and 4–8 June 2005).

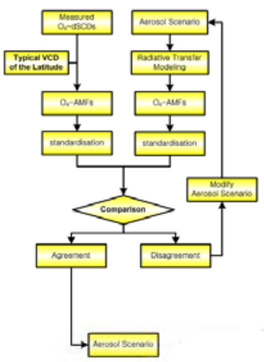

Fig. 5. Aerosol Retrieval Algorithm

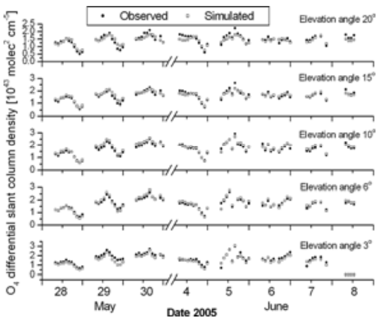

Fig. 6. Time series of observed and simulated O4 DSCD values obtained at EL = 3◦, 6◦, 10◦, 15◦, and 20◦ during measurement period (28–30 May and 4–8 June 2005).

RESULTS

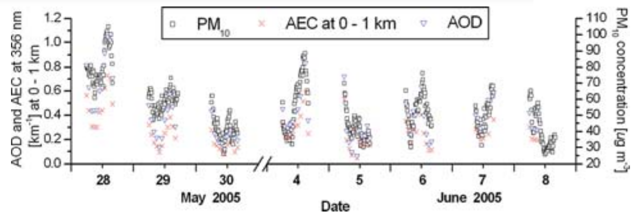

Fig. 7. Retrieved aerosol extinction coefficient (AEC) at 0–1 km height, aerosol optical depth (AOD), and surface PM10 concentration for measurement period (28–30 May and 4–8 June 2005).

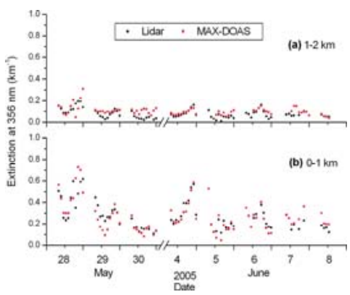

Fig. 8. Time series of hourly average aerosol extinction coefficient at 356 nm measured by MAX-DOAS and lidar for layers of and (a) 1–2 km and (b) 0–1 km.

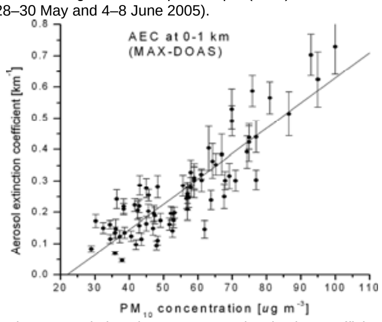

Fig. 9. Correlations between aerosol extinction coefficients (AECs) (km–1) and AOD from MAX-DOAS and surface PM10 concentration (*µg m–3*). *Error* bars represent errors estimated from retrieval covariance matrix.

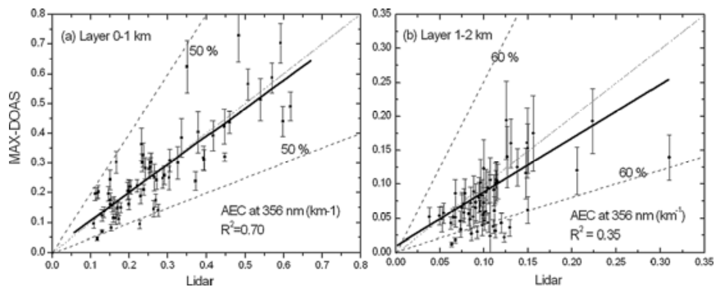

Fig. 10. Correlations between aerosol extinction coefficients (AECs) (km–1) from MAX-DOAS and lidar for measurement period (28–30 May and 4–8 June 2005) for layers of (a) 0–1 km.

REFERENCES

Irie, H., Kanaya, Y., Akimoto, H., Iwabuchi, H., Shimizu, A., and Aoki, K. (2008a). First Retrieval of Tropospheric Aerosol Profiles UsingMAX-DOAS and Comparison with Lidar and Sky Radiometer Measurements, *Atmos. Chem. Phys. 8:341–350*

Lee, C. K., Kim, Y. J., Tanimoto, H., Bobrowski, N., Platt, U., Mori, T., Yamamoto, K., and Hong, C. S. (2005). High ClO and Ozone Depletion Observed in the Plume of Sakurajima Volcano, *Japan. Geophys. Res. Lett. 32* L21809, doi:10.1029.2005GL023785.

Platt, U. (1994). Differential Optical Absorption Spectroscopy (DOAS) in Air Monitoring by Spectroscopic Techniques, in: M. W. Sigrist, ed., *Chemical Analysis, vol. 127, Wiley, New York, 27–83.*

SUMMARY and CONCLUSION

- To retrieve lower-tropospheric aerosol extinction coefficients, we applied an aerosol retrieval algorithm based on O4 SCD at a UVwavelength (356 nm), obtained from several MAXDOAS elevation angles.
-AECs obtained for the 1–2 km layer from MAX-DOAS are in agreement with lidar data within about 60%. We obtained a linear correlation coefficient (R2) of 0.35 between the two data sets for the 1–2 km layer at a UV wavelength (356 nm)
-This discrepancy can be attributed to several uncertainties, including the utilization of O4 absorption spectra in different wavelength regions, differences in lidar systems, and different atmospheric environment conditions during the measurement periods.